Journal of The Electrochemical Society

OPEN ACCESS

Analyzing the Aging Behavior of Lithium-Ion Cells Connected in Parallel Considering Varying Charging Profiles and Initial Cell-to-Cell Variations

To cite this article: Markus Schindler *et al* 2021 *J. Electrochem. Soc.* **168** 090524

Journal of The Electrochemical Society, 2021 **168** 090524

Analyzing the Aging Behavior of Lithium-Ion Cells Connected in Parallel Considering Varying Charging Profiles and Initial Cell-to-Cell Variations

Markus Schindler,[z] Philipp Jocher, Axel Durdel, and Andreas Jossen

Institute for Electrical Energy Storage Technology, Technical University of Munich, 80333 Munich, Germany

Aging behavior and long-term cell-to-cell variations have been much more frequently investigated in single-cells than cells connected in parallel. In particular, the literature lacks a study investigating the aging behavior of cells in parallel that is based on defined cell-to-cell variations and on the results of a previous single-cell aging study. Moreover, present studies are unable to exclude the impacts of measurement systems on their final results. To counter this deficiency, a novel 4-wire measurement technique is used which does not influence the current distribution but allows both single and parallel measurements to be recorded without changing the measurement configuration. Cells in parallel generally displayed improved aging behaviors in comparison to those seen in the single-cell aging study and the positive influence of extended CV-charging was evident, as long as the CV-charging phase was limited in length. It was also observed that the exclusion of critical voltage ranges exerted the most significant influence on the aging rate and dominates the influence of initial cell-to-cell variations in the long-term. As a result, it is recommended that module manufacturers reduce the effort spent on initial cell matching strategies for cells in parallel in favor of developing cell-specific charging profiles.

 [DOI: 10.1149/1945-7111/ac2089]

Manuscript submitted June 4, 2021; revised manuscript received August 6, 2021. Published September 21, 2021.

Manufacturing tolerances often result in initial cell-to-cell variations in the capacity and the internal resistance of lithium-ion cells.[1–12] Cell-to-cell parameter variations are found both within a production batch and between different production batches over the time span of the production process.[1,7]

Despite the strong possibility that battery modules would contain cells from only one batch Dubarry et al.[13] point out that every battery module is unique due to the unavoidable cell-to-cell parameter variations previously described. Presumably for this reason, researchers claim that care should be taken during the initial sorting process to build modules from cells that are as similar as possible[14–16] although an exact quantification of how similar they should be is not given. In combination with the finding that the aging behavior of single cells varies even with the same initial parameters,[4,17] the question arises of whether an acceptable level of variation should be defined or if initial sorting is worthwhile. For module manufacturers, the question is therefore, which initial cell-to-cell variations can be expected and tolerated as well as how initial deviations from the specified capacity or internal resistance affect the aging behavior of cells in parallel. For cells connected in serial, it has been shown that the cell with the lowest capacity is cycled the most, leading to a faster decrease in state of health SOH since each cell is charged or discharged using the same current in a series branch.[18,19] In contrast, an inhomogeneous current distribution normally occurs between cells connected in parallel.[7,16,20–22] Such inhomogeneous current distributions within a battery module can be caused by factors internal to the cell like by production variations in the thickness of electrodes or the weight fraction of active materials,[23–25] or due to cell-external reasons such as differing contact resistances or connection topologies.[3,16,20] In particular, the external factors mentioned indicate that a measurement setup may have an impact on the current distribution between cells in parallel, which in turn would affect the load profile of the individual cells.[26] Although it has been observed that differing load profiles usually lead to different aging behaviors of individual cells,[7,17] however, there are contrasting opinions in the literature as to whether initial cell-to-cell variations between cells connected in parallel lead to convergent[7,10,14,27] or divergent[7,25] aging behaviors.

Schuster et al.[10] analyzed cell-to-cell parameter variations of capacity and impedance from two sets of 954 cells from a battery electric vehicle and claimed that a continuous aging process leads to both an increase in cell-to-cell parameter variations and an uneven aging behavior of interconnected cells. In a similar vein, Baumann et al.[7] investigated parameter variations in two aged 96s2p battery modules. After disassembling the modules, further cycling was applied to ten 1s2p cell pairs for another 400 cycles. The findings showed that the spread of cell-to-cell parameter variations increases over the lifetime of the cells and that the state of inhomogeneity of the capacities of the cells in parallel increased during aging. By comparing distinct 1s2p cell pairs, they also showed that the spread of aging behavior between parallel pairs increases during aging.

An et al.[27] used cell-to-cell variations of cells with a nominal capacity (C_N) of 5.3 Ah for parametrization of Monte-Carlo simulations of an equivalent circuit model containing a cell with a nominal capacity of 3.35 Ah. They concluded that the cell-specific aging rate has a major influence on the aging behavior of cells in parallel. Simulations conducted by Gogoana et al.[14] showed that an initial difference in resistance of 20% would result in a decrease in lifetime of 40%. As a consequence, they suggest an internal resistance matching to reduce the SOH spread between the cells over their lifetime. Additionally, they recommended that the cells should not be charged to their maximum capacity to avoid harmful current peaks at the end of charging.[14] On the other hand, Baumhöfer et al.[12] claimed that the parallel connection of cells would help to reduce the aging spread between the cells, since the aging effects are averaged, while Santhanagopalan and White[25] showed that reducing initial cell-to-cell variations is one of the key factors in improving the lifetime of battery packs and decreasing the rejection rate when building them. The somewhat contradictory results of these studies may possibly be due to external factors such as distortions in the current distribution caused by the measurement setup and leading to altered aging behaviors.[26,28] Furthermore, adapted charging profiles have not been considered as possible factors leading to convergent aging behavior within cells in parallel. The literature also does not contain an aging study on cells connected in parallel which included the findings of an aging study on single cells from the same production batch. Accordingly, a coherent investigation of initial cell-to-cell variations as well as the aging behavior of both single cells and of cells connected in parallel all from the same production batch was deemed necessary.

[z]E-mail: markus.ms.schindler@tum.de

Table I. Specifications of the investigated cell INR18650MJ1, manufactured by LG Chem.

Parameter	Symbol	Specification
Min. nominal capacity[a)]	C_N	3.35 Ah
Lower voltage limit[a)]	U_{min}	2.5 V
Upper voltage limit[a)]	U_{max}	4.2 V
Max. charge current[a)]	$I_{Ch_{max}}$	3.35 A
Max. discharge current[a)]	$I_{DCh_{max}}$	10 A
Mean capacity[b)]	μ_C	3.43 Ah
Standard deviation of C[b)]	σ_C	12.4 mAh
Rel. coefficient of variation of C[b)]	κ_C	0.4%
Mean internal resistance[b)]	μ_R	28.9 mΩ
Standard deviation of R_i[b)]	σ_R	0.3 mΩ
Rel. coefficient of variation of R_i[b)]	κ_R	0.9%

a) data sheet.[31] b) measured.[1]

In the following we therefore present the first study that investigates the aging behavior of cells connected in parallel while considering two important aspects: first, the initial cell-to-cell variations of the cells,[1] and second, the investigation of charging profiles, which are based on the results of an existing aging study on single cells of the same production batch.[17] The first major finding from the single-cell aging study is that extended constant voltage (CV) charging resulted in a lower aging rate and smaller long-term cell-to-cell variations. The second is that the most significant effect on the aging rate and the long-term cell-to-cell variations was achieved by reducing the upper voltage limit during constant current-constant voltage (CC-CV)-charging. Building on these existing studies this work aims to answer the following research questions:

1. Does extended CV-charging also have a positive influence on the aging behavior of cells in parallel?
2. Does a reduced upper voltage limit also induce positive effects on cells in parallel?
3. With regard to reducing the aging of cells in parallel, is it more beneficial to sort by internal resistance or by cell capacity?
4. Can the influence of initial cell-to-cell variations in internal resistance or capacity be dominated by the influence of a reduced upper voltage limit and an initial cell matching thus be omitted?

Experimental

Cell under investigation.—We tested 28 commercial INR18650MJ1 lithium-ion cells manufactured by LG Chem. The cells were taken from a group of 160 cells from batch 2 (B_2) produced in 10/2017 and incorporate silicon-graphite (SiC) active material on the anode side and nickel-rich lithium nickel manganese cobalt oxide (NMC) as a cathode material.[1,29,30] The minimum nominal reversible capacity of the cells is given as 3.35 Ah by the manufacturer. According to the data sheet, the cell should be operated between the lower voltage limit U_{min} of 2.5 V and the upper voltage limit U_{max} of 4.2 V. The charging current $I_{Ch_{max}}$ and the discharging current $I_{DCh_{max}}$ should not exceed 3.35 A and 10 A, respectively. The specifications are summarized in Table I and were complied with in all of the studies in this paper.

Results of previous studies.—Three different batches of these cells were analyzed prior to this study. The results of the initial characterization are described in detail in Ref. 1. To allow comparison with the results of the single-cell aging study presented in Ref. 17, only cells of B_2 were used for the present study. Cells of B_2 showed a mean capacity μ_C of 3.43 Ah. The corresponding standard deviation σ_C amounted to 12.4 mAh which corresponds to a relative coefficient of variation κ_C of 0.4%. Regarding the cells impedance, the mean internal resistance μ_R, the standard deviation σ_R and the relative coefficient of variation κ_R amounted to 28.9 mΩ, 0.3 mΩ, and 0.9%, respectively. For the single-cell aging study presented in Ref. 17, cells of the reference study (P2B2, three cells) achieved between 537 equivalent full cycles (EFC) and 645 EFC at 80% SOH, which corresponds to a variation of 20.1% between the lowest and the highest number of EFC reached. Please note that the calculated number of EFC corresponds to the result if the cumulative charge throughput of the cell under investigation is divided by twice its nominal capacity, i.e., for the cell under investigation, one EFC therefore equals a charge throughput of 6.7 Ah. An extended CV-charging phase (P3B2, three cells) led to an increase in EFC between 646 and 700 EFC in a sample taken from the same batch, and a decreased cell-to-cell variation of 8.4%. Excluding critical voltage ranges by reducing the upper voltage limit to 4.089 V (P4B2, two cells) showed the most significant influence on both the total EFC and the variance between the cells. Consequently, this group of cells reached 847–850 EFC, which corresponds to a variation of 0.35%.

Preparation of the cells.—Since the cells were stored at 5 °C (50% state of charge (SOC)) for 2.5 years prior to this study, they were reactivated, reconditioned, and rescreened before they were matched for the studies conducted in this work. First, cells were stored within a climate chamber (Vötsch) for 6 h for thermal conditioning after storage. Subsequently, 5 conditioning cycles (BaSyTec, CTS) were performed using constant current CC-charge and -discharge steps. After a pause of 6 h, the following capacity checkup was conducted. The capacity C was determined by the sum of the CC- and the CV-discharge capacity measured in the second cycle of this step. Finally, the impedance Z of the cells was measured by electrochemical impedance spectroscopy (EIS) (Biologic, VMP3) at 50% SOC and the R_i evaluated at $\mathrm{Im}(Z) = 0$, the zero crossing of the imaginary part. The specifications of the different steps are summarized in Table II.

Measurement principles.—As discussed within our previous work,[26] the test bench and the measurement method can also affect the current distribution. Therefore, the "virtual parallel connection"[26] is

Table II. Sequence of the tests performed to investigate cell-to-cell variations. C was determined in step 3 by the sum of CC- and CV-discharge capacities in the second cycle. R_i was determined by an EIS at 50% SOC and evaluated at $\mathrm{Im}(Z) = 0$, the zero crossing of the imaginary part. Cells were cycled between 4.2 V and 2.5 V. I_{Ch-CV} and I_{Dch-CV} represent the absolute cell current limits of the corresponding CV phase. N_{FC} indicates the number of full cycles performed within the respective step. All tests were performed at an ambient temperature of 25 °C.

Step	Sequence	Duration	I_{Ch-CC}	I_{Ch-CV}	I_{Dch-CC}	I_{Dch-CV}	t_{pause}	N_{FC}
1	Thermal Conditioning	6 h	—	—	—	—	—	—
2	Conditioning Cycles	—	0.5 C	—	0.2 C	—	0.5 h	5
	Pause	6 h	—	—	—	—	—	—
3	Capacity Check	—	0.5 C	50 mA	0.2 C	50 mA	0.5 h	2
	Pause	6 h	—	—	—	—	—	—
4	EIS[a)]	—	—	—	—	—	—	—

a) $f \in$ [10mHz; 10kHz], $\hat{I}$ = 140 mA, 13/10/5 points per decade within [10 kHz;1 Hz]/[1 Hz;100 mHz]/[100 mHz;10 mHz].

Table III. Summary of the investigated studies. The entries below the reference study (Ref) specify the difference compared to the reference study, where—indicates that no change was made from the reference. I_{Ch-CC} and I_{Dch-CC} indicate the applied current rate per cell. I_{Ch-CV} represents the absolute cell current limit of the CV-charging sequence. All tests were performed at an ambient temperature of 25 °C.

Study Ref01/Ref02	I_{Ch-CC} 0.5 C	I_{Ch-CV} 100 mA	I_{Dch-CC} 1 C	U_{min} 2.5 V	U_{max} 4.2 V	dR —	dC —
CV01/CV02	—	33.5 mA	—	—	—	—	—
V01/V02	—	—	—	—	4.089 V	—	—
dR1S	—	—	—	—	—	σ_R	—
dR2S	—	—	—	—	—	$2\sigma_R$	—
dC1S	—	—	—	—	—	—	σ_C
dC2S	—	—	—	—	—	—	$2\sigma_C$
V-dR1S	—	—	—	—	4.089 V	σ_R	—
V-dR2S	—	—	—	—	4.089 V	$2\sigma_R$	—
V-dC1S	—	—	—	—	4.089 V	—	σ_C
V-dC2S	—	—	—	—	4.089 V	—	$2\sigma_C$

used. The virtual parallel connection negates the influences of inhomogeneous wiring, contact resistances, and additional sensors by using an integrated 4-wire measurement technique and exploits the communication capability (via a battery cycler) between the test channels connected in parallel to control the current distribution by solving Kirchhoff's laws. This measurement setup eliminates the need for additional sensors, such as hall or flux-gate sensors, to determine the current distribution, reducing the complexity of the setup. A shunt resistor, which would also influence the current distribution, is no longer required. The virtual parallel connection therefore offers two major advantages over previous studies. First, the current distribution, and consequently the aging behavior of the cells in parallel is not influenced by the measurement setup, for example, the influence of contact resistances is negated. Second, this method allows the cells to be cycled in parallel while allowing checkup routines to be performed on single cells requiring neither changes of the measurement configuration nor the physical disconnection of the cells. The virtual parallel connection therefore ensures that the aging behavior during cycling of the cells in parallel was unaffected by checkup routines carried out on single cells. Further details of the measurement procedure can be found in our previous work.[26]

Terminal boards were used to connect the cells with the cycler, including gold-plated spring contact pins (Feinmetall, F840) and 4-wire measurement technology. All cells were placed within a temperature chamber with an ambient temperature of 25 °C and it was ensured that the cells were not exposed to air flow from the fan. As a result, temperature gradients caused by the climate chamber were not expected.

Design of experiment.—This study examines the aging behavior of lithium-ion cells connected in parallel with reference to initial cell-to-cell variations. To this end, an initial cell matching (see Table IV) was carried out to select cells for the different aging studies using the C and R_i values determined during the cell preparation prior to the aging experiment. For the reference aging studies, where the cells displayed the smallest initial deviations in C or R_i, a maximum deviation in C of 1.80 mAh and in R_i of 0.04 mΩ were measured. This corresponds to relative deviations of 0.05% for C and 0.13% for R_i compared to the respective mean values μ_C and μ_R, deviations which are deemed to be small enough to neglect.

The cells of the reference studies (Ref01, Ref02) were connected in parallel and charged to 4.2 V, using a charging current of 0.5 C per cell. The subsequent CV-charging phase was terminated when the charging current fell below 100 mA. Afterwards, the cells were discharged at 1 C per cell to 2.5 V without CV-discharging. The influence of CV-charging (CV01 and CV02) and a reduced upper voltage limit (V01 and V02) were initially conducted on cells with negligible cell-to-cell variations. To examine the effects of initial deviations, cells were sorted so that they differed by one or two σ in either C or R_i. Since either C or R_i was varied for a given set of cells, this resulted in four additional studies named dR1S, dR2S, dC1S, and dC2S. Here dC indicates an initial deviation in C and dR an initial deviation in R_i. Suffixes 1S and 2S indicate the quantity of deviation as a multiple of σ. Since the single-cell aging study has shown that a reduced upper voltage limit had the greatest influence on the aging behavior, the influence of initial cell-to-cell variations of C or R_i in combination with a reduced upper voltage limit is additionally investigated. This leads to another four studies named V-dR1S, V-dR2S, V-dC1S, and V-dC2S. Table III summarizes the studies.

Checkup routines.—The development of the SOH was recorded during regular checkup routines at an ambient temperature of 25 °C. Capacity measurements to determine the SOH were performed using the profile described in Table II. As described above, the virtual parallel connection allows for checkup routines to be carried out on the single cells, without any changes to the measurement configuration or any need to disconnect the cells. The cell voltage limits were set to 2.5 V and 4.2 V for all studies, as recommended by the manufacturer. The applied charge I_{Ch-CC} and discharge I_{Dch-CC} currents as well as the cutoff current of 50 mA during CV-charging I_{Ch-CV} were chosen according to the manufacturer's data sheet. The cutoff criteria during CV-discharging I_{Dch-CV} was based on I_{Ch-CV}. This measurement procedure has been used by multiple authors.[1,17,18,32] Checkup routines on individual cells were undertaken every 50 cycles to track the aging behavior as accurately as possible without interrupting the specific process of cyclic aging occurring in the parallel connection too often. According to the data sheet of the cells, the aging rate is increased during the first 50 cycles which is why an additional checkup routine is performed after 25 cycles.

End of experiment.—The fulfillment of either of two different criteria were chosen to signal the end of a study. First, cycling of the parallel cells was terminated when the SOH of a single cell dropped to 80%. In this study, the SOH is calculated individually for each cell by dividing the current capacity by the initial capacity and expressing the result as a percentage. Second, the study was ended when a cell reached more than 537 EFC. This number of EFC corresponds to the number of EFC reached by the cell with the highest aging rate in the reference study of the single-cell aging study at 25 °C (P2B2).[17]

Evaluation.—Since the aging rates measured in both single cells and cells in parallel can differ even between comparable studies, a reference study must be chosen or a reference value calculated to allow for the comparison of results. In the opinion of the authors, averaging the aging rates of different studies would smear the individual aging rates and hamper a detailed discussion which is why a specific aging study is preferred as a reference. Since the

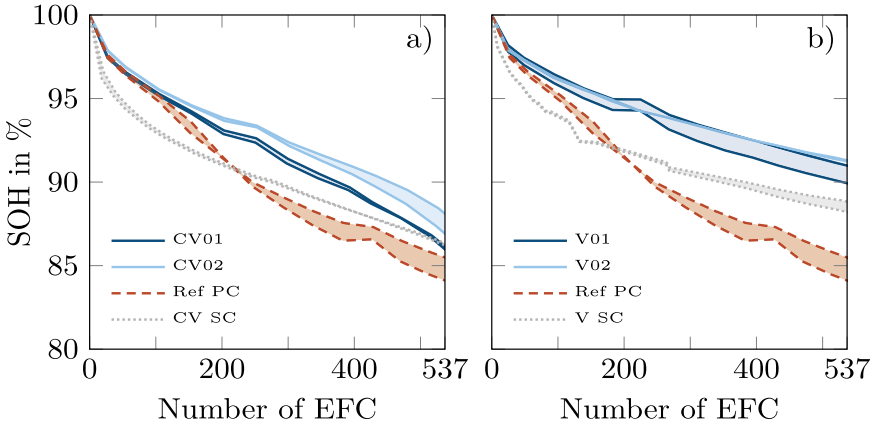

Figure 1. Influence of extended CV-charging and a reduced upper voltage limit (blue, solid) on the aging rate compared to the reference study Ref PC (red, dashed) and the respective single-cell aging CV SC (gray, dotted) from Ref. 17. a) Extended CV-charging. b) Reduced upper voltage limit.

components with the shortest lifetime are critical to avoid regress claims, the limiting cell or module is decisive for manufacturers of battery modules. The end-of-life of a battery system is therefore determined by the cell or the module with the highest aging rate.[18] For this reason, we chose study Ref PC 02 as the reference in the following, which displayed an increased aging rate compared to Ref PC 01, as can be seen in Fig. A·1. Furthermore, by comparing the aging rates of the cells in parallel with the cell with the lowest and highest aging rates from the single-cell aging study, a comprehensive comparison with previous investigations should be possible. In the single-cell aging study, the cell with the highest aging rate reached 80% SOH at 537 EFC,[17] which is the source of the first termination criterion. Therefore, the aging rate of each cell is linearly interpolated between the checkup before and after the limit of 537 EFC and the resulting SOH is calculated.

Limitations.—Inhomogeneous cell heating caused by unequal contact resistances of the cells in parallel would probably lead to uneven aging behavior.[17] Such inhomogeneous contact resistances are unlikely to appear in the chosen setup but would not be detected by the virtual parallel connection.

Results

The following results show the aging rates of the different studies as compared to the reference study of cells in parallel (Ref PC, red, dashed) as well as to their respective single-cell aging study (Ref SC, CV SC, V SC, gray, dotted). The results described within this section are summarized in Fig. 7 at the end of the discussion.

Figure 1a) illustrates the aging behavior of the study analyzing the influence of an extended CV-charging. Up to approx. 100 EFC, CV01 and CV02 show an almost identical aging behavior to Ref PC. Thereafter, CV02 displays a lower aging rate than CV01 up to approx. 400 EFC. From 400 EFC, the aging rates of CV01 and CV02 increase, with a transition to nonlinear aging rates already emerging for both studies toward the end of the experiment. Compared to Ref PC, CV01 and CV02 display lower aging rates after 100 EFC, resulting in a smaller decrease in SOH. However, due to increased aging rates from about 400 EFC, the SOH of cells from CV01 and CV02 approaches that of the cells from Ref PC again by the end of the experiment. This leads to deviations in SOH between CV01 and Ref PC of 0.5% and of at least 1.4% between CV02 and Ref PC. Focusing on the SOH deviation within cells from CV01 or CV02, a spread between the cells from CV01 occurs from 200 EFC on, which decreases again up to 400 EFC. No significant deviation occurs between the cells from CV01 above 400 EFC, resulting in a SOH spread of 0.2% at the end of experiment. Similarly, no deviation between the SOH of the cells in CV02 can be detected before 200 EFC. However, from 200 EFC an increasing SOH spread can be detected, leading to a maximum deviation of 1.2% at the end of the experiment which is slightly below the SOH spread of 1.4% of the cells from Ref PC. Comparing the aging trends of the cells connected in parallel within both CV01 and CV02 with the respective single-cell aging behavior of CV SC (P3B2[17]), CV01 and CV02 display a smaller SOH decrease up to about 510 EFC before the SOH of CV01 falls below the SOH of CV SC until the end of the experiment. For CV02, the SOH of both cells is above CV SC at the end of the experiment.

Figure 1b illustrates the aging trends of studies V01 and V02 which display the influence of a reduced upper voltage limit for cells in parallel compared to Ref PC and the respective single-cell aging study V SC from Ref. 17. As with CV01 and CV02, V01 and V02 display their highest aging rates for the first 25 EFC. Qualitatively, the aging process can be divided into three areas. The highest aging rate for all cells occurs bellow 25 EFC. The aging rate subsequently decreases until approx. 220 EFC. From 220 EFC to the end of the experiment, the aging rate reduces further. Compared to Ref PC, the smaller aging rates of V01 and V02 result in a significantly reduced decrease in their SOH from 25 EFC until the end of the experiment. This results in a final SOH that in comparison to that of Ref PC is at least 4.4% higher in the cells from V01 and at least 5.8% higher in the cells from V02. Analyzing the SOH development within V01, a maximum SOH deviation of 1.1% occurs at the end of the experiment. This deviation is greater than the SOH deviation of 0.1% between the cells from V02, but less than the deviation of 1.4% between the cells from Ref PC. Comparing the aging behavior of the cells in parallel within V01 and V02 with the respective single-cell aging study V SC, all of which possessed an upper voltage limit of 4.089 V (P4B2[17]), a decreased aging rate can be detected for cells in parallel within the first 25 EFC. As until approx. 175 EFC the aging rate of the cells in parallel was lower than that seen in the single-cell aging study, the SOH of the cells in parallel was consistently higher than that of the single-cell aging study. From 175 EFC to the end of the experiment, the aging rates of the cells in parallel and the respective single cells are similar, which is the cause of the almost identical SOH evolution. This leads to a final SOH increase of at least 1.1% for cells from V01 and of at least 2.4% for cells from V02 compared to the respective single cells.

Figure 2a illustrates the aging trends measured in studies dR1S and dR2S analyzing the influence of initial cell-to-cell variations in cell's internal resistance between the cells in parallel compared to Ref PC, which contains no significant initial deviations, and the respective single-cell aging study Ref SC. The previously observed increased aging rate within the first 25 EFC is also present for dR1S and dR2S. Subsequently, dR2S displays an increased aging rate as compared to dR1S until approximately 250 EFC. Thereafter, the

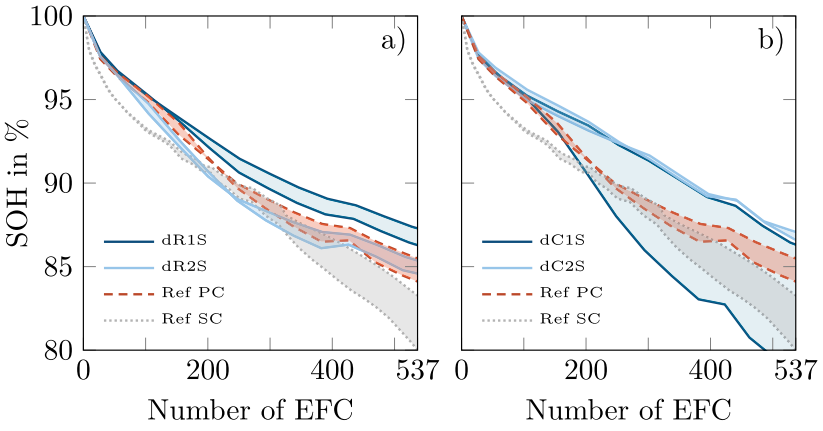

Figure 2. Influence of initial cell-to-cell variations between the cells in parallel (blue, solid) compared to the reference study Ref PC (red, dashed) and the respective single-cell aging Ref SC (gray, dotted). a) Initial difference in internal resistance of 1σ (dR1S) and 2σ (dR2S). b) Initial difference in capacity of 1σ (dC1S) and 2σ (dC2S). Please note that the study dC1S was terminated when one of the two cells in parallel reached the 80% SOH limit, as defined in the study design.

SOH of dR1S and dR2S decrease equally until the end of the experiment. Compared to Ref PC, the aging trend of dR1S shows a lower aging rate, which is why the SOH of the cells in dR1S is consistently above the SOH of Ref PC from 25 EFC onwards. At the end of the experiment, this results in a dR1S SOH between 0.8% and 1.8% higher than the best-performing cell from Ref PC. dR2S displays consistent aging behavior with that of Ref PC up to about 75 EFC. Subsequently, dR2S shows a higher aging rate than Ref PC, causing the SOH of the first cell from dR2S to fall below that of Ref PC at 300 EFC and the second cell from dR2S to fall below the lowest SOH shown by Ref PC at 450 EFC. At the end of the experiment, the SOH of the cells from dR2S is between the SOHs of Ref PC. Compared to the cell with the highest SOH in Ref PC, the SOH of the dR2S cells is 0.1% and 0.9% lower at the end of the experiment. The progression of the SOH begins to diverge from around 150 EFC for cells from dR1S and for cells from dR2S from about 220 EFC. In both cases, the deviations increase until the end of the experiment, which leads to respective final SOH spreads of 0.8% and 1.0% for cells from dR1S and dR2S compared to 1.4% for cells from Ref PC. Comparing the aging behavior of cells connected in parallel displaying initial deviations in internal resistance with the corresponding single-cell aging (P2B2[17]), a lower aging rate is observed for dR1S over the entire experiment, leading to a SOH increase of at least 3% and 4% for the cells from dR1S at the end of the experiment. For dR2S, the SOH is initially above Ref SC until 200 EFC, and the curves almost coincide between 200 and approx. 300 EFC. Due to the lower aging rates of the cells from dR2S above 300 EFC, a SOH deviation between the cells from dR2S and Ref SC of at least 1.3% and 2.1% develops by the end of the experiment.

Figure 2b illustrates the aging trends of studies dC1S and dC2S analyzing the influence of initial cell to cell variations in cell capacity between the cells in parallel compared to Ref PC, which does not contain significant initial deviations, and the respective single-cell aging study Ref SC. Up to 25 EFC, an increased aging rate is present for dC1S and dC2S. Subsequently, the aging rates of dC1S and dC2S are at a comparable level up to approx. 150 EFC. From about 150 EFC, one cell from dC1S shows a significantly increased aging rate leading to a comparatively steep SOH drop. The second cell from dC1S does not show this anomaly and its aging trend is widely consistent with that of the cells from dC2S. Overall, the SOHs deviate by 7.7% for dC1S and by 0.5% for dC2S from the reference values at the end of the experiment. Due to the increased aging rate of one cell from dC1S, a SOH difference of 7.0% occurs between the cells with the lowest SOH from dC1S and the highest SOH from Ref PC at the end of the experiment. The SOH of the second cell from dC1S is at least 0.7% greater than Ref PC. Compared to Ref PC, the aging rates of dC2S are at a similiar level until 150 EFC. From 150 EFC onwards, the aging rates of dC2S are decreased, which leads to a smaller SOH decrease for cells from dC2S compared to Ref PC. However, at the end of the experiment, there is only a SOH deviation of 1.1% and 1.6% between the cells from dC2S and the cell with the higher SOH from Ref PC. Comparing the aging behavior of cells connected in parallel which display initial deviations in cell capacity with the corresponding single-cell aging (P2B2[17]), only the SOH of the cell from dC1S with the highest aging rate has a SOH 1.5% lower than Ref SC at the end of the experiment. The SOH of the second cell from dC1S and the SOH from both cells from dC2S is greater than Ref SC by at least 2.9%, 3.3%, and 3.8%, respectively.

Figure 3 illustrates the aging trends of studies V-dR1S and V-dR2S, analyzing the influence of initial cell-to-cell variations in a) internal resistance or b) capacity in combination with a reduced upper voltage limit as compared to Ref PC (which is effectively deviation-free) and the respective single-cell aging study V SC. A larger SOH decrease within the first 25 EFC, previously observed for all other studies, also occurs with a limited upper voltage limit combined with either initial differences in internal resistance or capacity. Additionally, studies with an initial cell-to-cell variation of one standard deviation, i.e., V-dR1S and V-dC1S, display a lower aging rate compared to the aging studies with an initial deviation of two standard deviations, i. e., V-dR2S and V-dC2S. A smaller decrease in SOH for V-dR1S and V-dC1S is also evident. Compared to Ref PC, V-dR1S, V-dR2S, V-dC1S, and V-dC2S display lower aging rates after 25 EFC, which in turn lead to a smaller decrease in SOH for these studies. Consequently, the SOH of both cells from V-dR1S is 5.7% greater than Ref PC. For the cells from V-dR2S, the SOH is 3.3% and 5.2% greater than Ref PC. For the cells from V-dC1S, an initial difference in the cells' capacities combined with a reduced upper voltage limit resulted in a SOH 4.2% and 5.8% greater than Ref PC at the end of the experiment. For V-dC2S, the SOHs are 1.5% and 3.0% greater than that of Ref PC. Analyzing the long-term deviations between the cells in parallel within the studies V-dR1S, V-dR2S, V-dC1S, or V-dC2S, no significant deviation develops between the cells from V-dR1S over the entire experiment which is why an end-of-experiment deviation of 0.0% was calculated. On the other hand, a deviation in SOH develops for V-dR2S which starts to increase at 25 EFC, leading to a maximum deviation of 2.3% at the end of the experiment. For V-dC1S, a deviation in the SOH develops from about 180 EFC, increasing steadily to a maximum deviation of 1.5% at the end of the experiment. A SOH

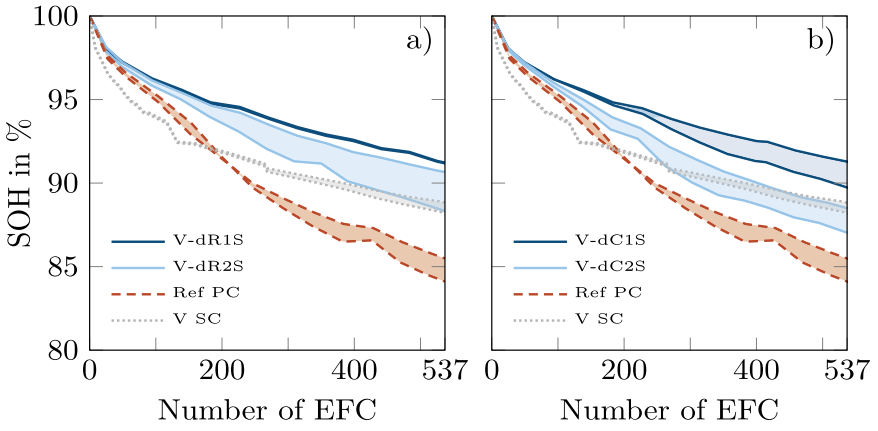

Figure 3. Influence of reduced upper voltage limit in combination with initial cell-to-cell variations between the cells connected in parallel (blue, solid) as compared to the reference study Ref PC (red, dashed) and the respective single-cell aging study V SC (gray, dotted). a) Initial difference in internal resistance of 1σ (V-dR1S) and 2σ (V-dR2S). b) Initial difference in capacity of 1σ (V-dC1S) and 2σ (V-dC2S).

spread between the cells from V-dC2S develops from 25 EFC, increasing to 1.5% at the end of the experiment; a comparable deviation to that of V-dC1S. Comparing the aging rates of V-dR1S, V-dR2S, V-dC1S, and V-dC2S with the respective single-cell aging study V SC, both V-dR1S and V-dC1S show lower aging rates, resulting in an increased SOH for both cells from V-dR1S of at least 2.4% as well as of 0.9% and 2.5% for cells from V-dC1S at the end of the experiment. For V-dR2S, the SOH of one cell is 1.9% larger than V SC, whereas the SOH of the second cell ends between the SOHs of the cells from V SC. For V-dC2S, the SOH of one cell ends between the SOHs of V SC and the second cell ends with an SOH at least 1.2% lower than V SC.

Discussion

Loss of capacity at an increased rate during the first 25 to 50 EFC is an expected aging behavior referred to within the data sheet of the cell.[31] As can be seen from Figs. 1–3, this increased capacity loss is also seen in the aging behavior of cells in parallel. However, the aging rate is decreased for cells in parallel compared to the single cell. The reason for the decreased aging rate of cells in parallel is hard to identify with certainty in the basis of the recorded measurement data. A possible explanation can be given based on the current distribution between the cells from the reference study Ref PC, illustrated in Fig. 4. The initial cell matching by capacity and internal resistance results in an almost homogeneous current distribution at the beginning of the discharge. However, the current deviates inhomogeneously between the cells in the longer term which indicates an inhomogeneous development of the cell impedances and open-circuit-voltage (OCV) levels.[7,16,20–22] Ludwig et al.[33] showed that such dynamic changes of cell's impedance are to be expected during a complete discharge. Since the dynamic cell impedances and OCV levels can develop differently, the parallel connection of the cells causes a dynamic distribution of the discharge current in a ratio commensurate to that of the impedances and the differences in OCV levels. This in turn means that a cell in parallel with a second cell can be discharged with a higher current if its dynamic cell impedance and OCV level is below that of the second cell at a given point in time, but that these circumstances are dynamically adapted.[21,34] As illustrated in Fig. 4, this leads to a repeated change of the current distribution between the cells. Compared to a CC-discharge of a single cell, cells in parallel can interact and support each other to share the current load dynamically, which can lead to reduced current densities in the active materials of the cells in parallel. The locally reduced current density would in turn correspond to a locally reduced stress in the active material,[35,36] which should result in a lower aging rate for cells in parallel, as displayed within Figs. 1 to 3.

A decreased CV-charging cutoff current causes the cells in parallel to be exposed to voltage levels of 4.2 V for longer periods, which encourages side reactions, especially at the NMC-811 cathode.[30,37] Increased side reactions should in turn give rise to accelerated aging behavior. However, the SOH development of CV01 and CV02 display higher SOH than the reference study Ref PC, as can be seen in Fig. 1a. Consequently, the influence of additional side reactions of NMC-811 particles during extended CV-charging, which would increase the aging rate, seems to be diminished by another effect of extended CV-charging. This can be explained by the findings of Richter et al.[38] They described that for C-rates above 0.1 C (as used within these studies, see Table III), graphite particles are preferentially lithiated compared to silicon particles, which results in inhomogeneous lithiation between these materials at the end of CC-charging. Richter et al.[38] stated that this inhomogeneity is reduced in the subsequent relaxation phase as lithium migrates from graphite to silicon. These balancing effects cause a more homogeneous lithiation of the silicon and graphite particles within the anode active material, which is induced within this study by the extended length of the CV-charging and seems to have a positive influence on the aging rate for the material combination used. Consequently, a possible explanation for the increased SOH of cells from CV01 and CV02 is that due to the more homogeneous lithiation, single particles of graphite and silicon are more uniformly delithiated in the subsequent discharge phase and thus the local aging rate is reduced on the anode side. Furthermore, as can be seen in Fig. 1 by comparing the spreads between the cells from CV01 and CV02 as compared to Ref PC, the long-term evolution of cell-to-cell variations is also reduced for cells in parallel by an extended CV-charging. On the other hand, the increased aging rates for CV01 and CV02 starting at around 400 EFC indicate the onset of nonlinear aging behavior, provoked by increasing CV-charging times as shown in Fig. 5. This can be clearly seen in the steady increase of the length of the CV-charging sequence for cells from CV01 and CV02 from 1.1 h at the beginning to 3.5 h at the end of the experiment which is considerably greater than Ref PC (0.9 h to 1.7 h) and CV SC (0.9 h to 1 h). Although CV-charging was limited to 1 h for CV SC in Ref. 17. This was not the case for the cells aged in parallel. This extended CV-charging at 4.2 V leads to additional side reactions in the cathode active material, which appears to cancel out the positive effect within the anode active material as the number of EFC increases and can even cause nonlinear aging behavior. Consequently, the results of this study indicate that an extended CV-charging can have a positive influence on the aging behavior and the long-term evolution of cell-to-cell variations of cells in parallel which incorporate a silicon-graphite anode, provided that the length of the CV-charging sequence is limited in time and does not increase steadily with decreasing SOH.

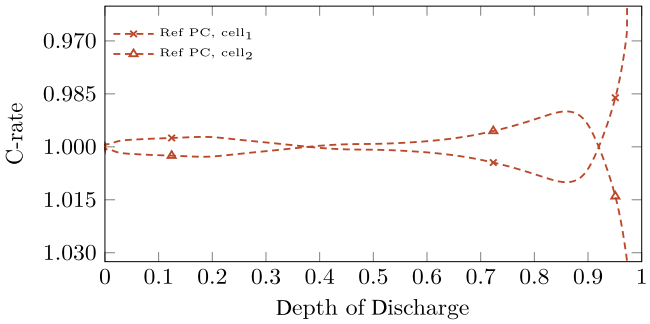

Figure 4. Current distribution between the cells of Ref PC at the beginning of the experiment (cycle 2). An initial cell matching ensured that initial cell-to-cell variations were reduced as much as possible.

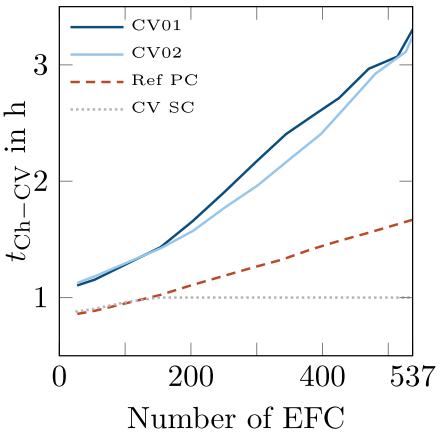

Figure 5. Duration of the CV-charging sequence t_{Ch-CV} in h. For cells in parallel t_{Ch-CV} increases steadily whereas t_{Ch-CV} of CV SC was limited to a maximum of 1 h in Ref. 17.

The positive effect of a reduced upper voltage limited was initially proved in Ref. 17 for single cells from the same production batch. A reduced upper voltage limit therefore leads to reduced aging rates on both anode and cathode side, while simultaneously reducing the extractable cell capacity by less than 3% for cyclic aging. As described above, silicon and graphite particles are lithiated simultaneously at lower C-rates (0.1 C and below) on the anode side.[38,39] However, at higher C-rates, the lithiation of graphite particles is preferred to silicon,[38–40] which should be the case within V01 and V02 as C-rates of 0.5 C per cell are applied during CC-charging. Accordingly, since the anode active material is not fully lithiated within V01 and V02 due to the reduced upper voltage limit, the volumetric expansion of the silicon particles in particular, is expected to be lower than in Ref PC. Consequently, the reduced particle swelling leads to less intense degradation of the anode active material[39] and a higher remaining amount of usable lithium,[41] which in turn increases the remaining capacity and as such, the remaining SOH within V01 and V02 by at least 4.4% and 5.8% above that of Ref PC, as seen in Fig. 1b). On the cathode side, reducing the upper voltage limit also reduces the swelling of the NMC particles,[30,42] but more importantly, critical phase transitions are at least partially avoided within the high-energy NMC active material.[37] Thus, the aging rate on the cathode side is also expected to be decreased in V01 and V02 in comparison to Ref PC. Moreover, as displayed in Fig. 1b, this leads to decreased cell-to-cell variations between the cells from V01 and V02 compared to that of Ref PC. As a result, limiting the volumetric expansion of silicon and avoiding critical voltage ranges of the NMC-811 cathode material by reducing the upper voltage limit can be seen as a promising method to extend the lifetime and decrease cell-to-cell variations of cells in parallel.

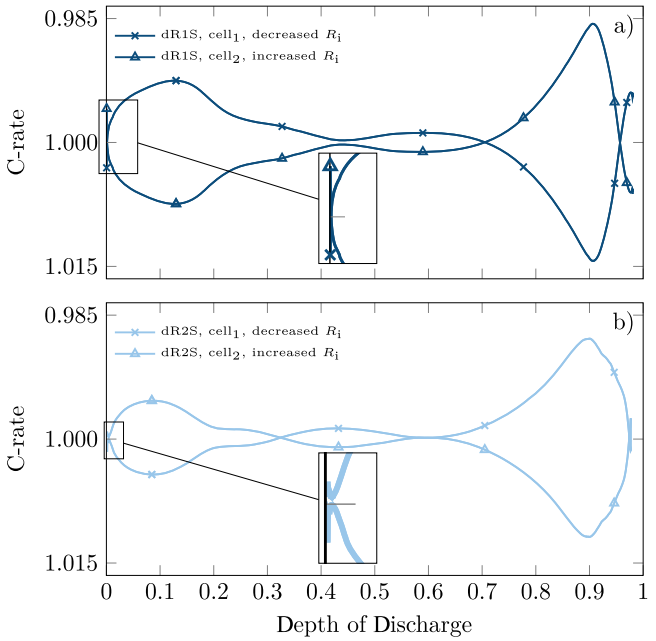

Figure 6. Current distribution between the cells of a) dR1S and b) dR2S at the beginning of the experiment (cycle 2). Due to an initial cell matching, the cells of dR1S differed by 1σ and the cells of dR2S by 2σ in internal resistance.

If cells are cycled at the same ambient temperature, the aging behavior of a cell is mainly influenced by the charge and discharge profile, the chosen voltage limits, and the charge throughput.[17,32] Since the cells in parallel were always operated within the same climate chamber and under equal voltage limits, the ambient temperature and the chosen voltage limits can be excluded as a reason for different aging behavior within this study. However, due to a possible inhomogeneous current distribution between the cells in parallel, the different charge and discharge currents applied to the cells may result in uneven charge throughput for these cells, provoking inhomogeneous aging rates and inhomogeneities in the SOH developments. Initial cell-to-cell variations in internal resistance or capacity are expected to cause such inhomogeneous current distribution between the cells in parallel.[21,28,34,43] At the beginning of the discharge, the current should divide between the cells in parallel according to their impedance ratios.[28,44] Consequently, the cell with the lowest initial internal resistance would therefore be discharged with a higher current at first.[20] During this time, the SOC of this cell decreases more rapidly, leading to a reduction in both impedance[33] and OCV level which in turn increases the discharge current.[21,22,28,34,44] This ideal behavior was also observed at the beginning of the discharge for studies dR1S and dR2S, as shown in Figs. 6a and 6b. However, the cell with the initially increased internal resistance was loaded with a higher current after only a few seconds in dR1S (see Fig. 6a), which contradicts the idealized current distribution. A modified current distribution can be caused by differences between both the impedances of the cells and the differences between their OCVs making it likely that an interaction of these factors caused the measured current distribution. In addition, the results of Ludwig et al.[33] show that cell impedance values are lowest in the range of 50% SOC, and significantly higher at high and low SOC. Since the cells were matched with reference to their impedance at 50% SOC, it is conceivable that the discrepancy in impedance between the cells may change at extremes of SOC. This is expected to be particularly relevant at 100% SOC when discharge begins. Initial cell-to-cell variations in internal resistance are therefore only one of multiple factors that contribute to an inhomogeneous current distribution.[7,16,20–22,34] Other factors are for example, deviations in the open-circuit-potentials,[44] differing entropy[45] and hysteresis behaviors, as well as dynamic changes to the cells' overpotentials[34] which lead to deviation of the current distribution from the idealized case.[7,16,21,22] Moreover, as shown in

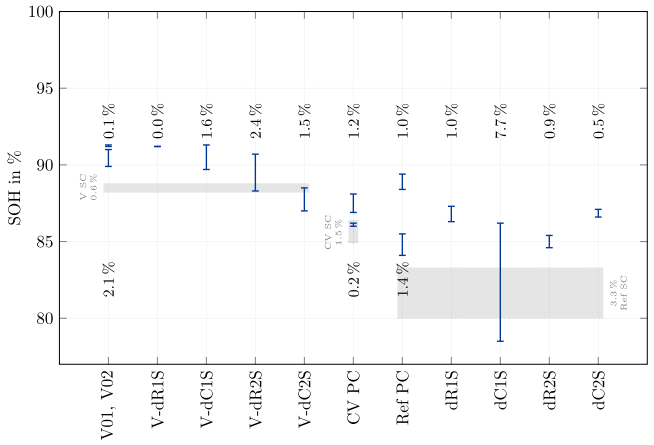

Figure 7. Summary of the results obtained from the different aging studies. Therefore, a reduced upper voltage limit displays the greatest influence on both the lifetime of the cells in parallel and the long-term cell-to-cell variations. Grey shaded areas display the final SOHs and cell-to-cell variations of the respective single-cell aging study V SC, CV SC and Ref SC. Additional numbers within the figure indicate the SOH difference between the cells of the respective study.

Fig. 6, the current distribution changes during cyclic aging, which is caused by varying contributions of the named factors.

Explaining the reasons and the driving forces of a changing inhomogeneous current distribution is out of the scope of this investigation but is the subject of ongoing research. The focus in this work is on the effects of initial cell-to-cell variations on the aging behavior of cells in parallel. Except for the named outlier within dC1S, the SOH of cells in parallel is within the range of Ref PC (dR2S) or better (dR1S, dC2S) as can be seen in Fig. 2. Consequently, the aging behavior of cells with initial cell-to-cell variations displays a similar or lower aging rate compared to Ref PC and a lower aging rate than Ref SC. Additionally, cells in parallel with initial internal resistance or capacity variations showed lower long-term cell-to-cell variations than Ref PC and Ref SC. To assess whether an initial cell matching by internal resistance or by capacity is preferable, two further aspects should be considered. First, it should be investigated whether there are significant differences between the aging behavior of the dR- and dC-studies. Second, which cell-to-cell variations have been studied in the literature and how does this affect the probable dR- and dC-scenarios. In answer to the third question, the final SOHs of cells from dC2S (87.1%, 86.6%) and cells from dR1S (87.3%, 86.3%) were comparable, while the final SOHs of cells from dR2S (85.4%, 84.6%) were only slightly lower. Due to the outlier from dC1S, the apparent slight gain from matching by resistance (leads to dC) may be unreliable. Additionally, we have shown in our previous work that cell manufacturers appear to use the capacity as the decisive factor for initial cell matching after cell production,[1] which is why greater variations in internal resistance than in capacity are to be expected during module assembly. Consequently, since cell manufacturers seem to initially match the cells by capacity before delivery and the observed aging behavior neither indicates a clear benefit to matching by internal resistance (leads to dC) nor to matching by capacity (leads to dR), the benefit of an additional matching prior to module assembly is disputable for cells connected in parallel as long as the relative coefficients of variations are small.

In the following paragraph, the influence of a reduced upper voltage limit on the aging behavior and the long-term cell-to-cell variations in the presence of initial cell-to-cell variations in internal resistance or capacity is discussed. Regarding the long-term cell-to-cell variations, only the extremely low deviation between the cells from V-dR1S suggests that a reduced upper voltage limit would be beneficial as appeared to be the case for V01, V02, and V SC. For V-dR2S, V-dC1S, and V-dC2S the long-term cell-to-cell variations were in the range of

Table IV. Initial cell-to-cell variations between the cells in parallel within the different studies. $R_{i,ini}$ and C_{ini} represent the absolute values of the initial internal resistance and the initial capacity respectively. $R_{i,ini}$ was measured by EIS at 50% SOC and evaluated at $\mathrm{Im}(Z) = 0$, the zero crossing of the imaginary part. C_{ini} was determined by the sum of the CC- and the CV-discharge capacity. dR and dC represent the initial difference in internal resistance or capacity after cell matching between the cells in parallel. The standard deviations σ_R and σ_C correspond to absolute values of 0.3 mΩ and 0.0124 Ah.[1]

Study	$R_{i,ini}$ in mΩ	C_{ini} in Ah	dR in mΩ	dC in Ah
Ref01	28.62	3.403	0.04	0.000
	28.66	3.403		
Ref02	28.43	3.374	0.00	0.001
	28.43	3.375		
CV01	28.89	3.386	0.04	0.000
	28.93	3.386		
CV02	28.56	3.374	0.00	0.002
	28.56	3.376		
V01	28.74	3.415	0.00	0.002
	28.74	3.417		
V02	28.53	3.375	0.03	0.001
	28.50	3.374		
dR1S	28.47	3.401	0.26	0.000
	28.73	3.401		
dR2S	28.24	3.403	0.51	0.000
	28.75	3.403		
dC1S	28.88	3.383	0.00	0.016
	28.88	3.399		
dC2S	29.01	3.379	0.02	0.029
	29.03	3.408		
V-dR1S	28.69	3.372	0.27	0.000
	28.42	3.372		
V-dR2S	28.14	3.398	0.54	0.000
	28.68	3.398		
V-dC1S	28.83	3.395	0.02	0.013
	28.85	3.382		
V-dC2S	28.72	3.413	0.02	0.026
	28.70	3.387		

Ref PC or slightly above. As such, neither a positive nor a negative influence on the long-term cell-to-cell variations can be attributed to a reduced upper voltage limit, if initial cell-to-cell variations were present. However, with respect to the aging rates and SOHs at the end of the experiment, a significant influence of a reduced upper voltage limit toward increased SOHs can be identified. This is quantified by the final SOHs for all studies with initial cell-to-cell variations and a reduced upper voltage limit which were increased by 1.5% (V-dC2S) and 5.7% (V-dR1S) versus the final SOH of Ref PC. Additionally, comparing the final SOHs between V-dR and V-dC, the final SOHs of V-dR are slightly above those of V-dC, which would indicate better results from initial matching by capacity (leads to dR) instead of an initial matching by internal resistance (leads to dC), as described above. More important, however, is the finding that, even in the presence of initial cell-to-cell variations, a reduced upper voltage limit resulted in a significant increase in the final SOHs for V-dR1S, V-dR2S, V-dC1S, and V-dC2S compared to the final SOHs of Ref PC, dR, and dC. As a result, with respect to the aging behavior, the influence of a reduced upper voltage limit dominates the effects of initial cell-to-cell variations. Thus, an additional cell matching can be neglected for cells in parallel if the upper voltage limit is reduced and the relative coefficients of variation are small, which with 0.4% and 0.9% for κ_C and κ_R respectively, was true for this study. Figure 7 summarizes the results obtained from the different aging studies and shows again, that a reduced upper voltage limit has the greatest impact on the lifetime and the long-term cell variations of the investigated cells.

Conclusions

Various studies were performed to investigate the aging behavior of cells connected in parallel which incorporate SiC anodes and nickel-rich NMC-811 cathodes, depending on the charging profile and with respect to initial cell-to-cell variations in internal resistance or capacity. The results of our previous study analyzing cell-to-cell variations[1] were used to select cells for the different aging studies with either no initial cell-to-cell variations from the mean, or a variation of one or two standard deviations in internal resistance or capacity. The charging profiles were taken from the aging study on single cells, presented in Ref. 17. In total, 14 aging studies were performed to analyze the influence of extended CV-charging and a reduced upper voltage limit as well as the influence of initial cell-to-cell variations on the lifetime and the long-term cell-to-cell variations of cells in parallel.

In general, a decreased aging rate was observed for cells in parallel compared to the respective single-cell aging study, leading to increased SOHs at the end of the experiment for cells in parallel. Initially, extended CV-charging resulted in a decreased aging rate for the cells in parallel. However, the aging rate increased along with the number of EFC and the initially positive effects faded, whilst the SOH approached or even fell below the SOHs from the reference studies of cells in parallel and single cells. The reason for this was identified as the continuously increasing duration of the CV-charging sequence from 1.1 h at the beginning to 3.5 h at the end of the experiment, far exceeding the 1.0 h CV-charging time in the single-cell aging study. Since the cells in parallel were exposed to voltage levels of 4.2 V for durations of up to 3.5 h during CV-charging, this probably accelerated degradation mechanisms within the nickel-rich NMC-811 cathode material, leading to an increased aging rate. Compared to the single-cell aging study, no effects could be observed for the long-term cell-to-cell variations of cells in parallel. Consequently, for the investigated cell with a silicon-graphite anode and with respect to the first research question, it can be summarized that an extended CV-charging can positively influence the aging behavior of cells in parallel, if the length of CV-charging is limited in time.

Compared to the respective single-cell aging study, reducing the upper voltage limit resulted in a further increase of the cell's SOH at the end of the experiment. Thus, reducing the upper voltage limit was confirmed as the most effective method for decreasing long-term cell-to-cell variations and increasing the lifetime of the cells. Regarding the second research question, reducing the upper voltage limit was proven to exert a positive influence on the aging behavior and the long-term cell-to-cell variations even for cells in parallel.

If an initial cell matching was omitted, the aging behavior of the studies incorporating initial cell-to-cell variations in internal resistance or capacity differed only slightly from the aging behavior of the reference study which did only contain negligible initial cell-to-cell variations. Combined with the findings from previous investigations that the capacity appears to be the decisive criterion used by cell manufacturers for initial cell matching prior to product delivery, an additional cell matching prior to module assembly cannot be justified based on the results in this work. This result is also supported by the fact that, compared to the aging behavior of the single cells, even initial cell-to-cell variations of two standard deviations (0.6 mΩ/24.8 mAh, 1.8%/0.8%) displayed a lower aging rate and reduced long-term cell-to-cell variations when connected in parallel. Regarding the third research question, provided that low initial cell-to-cell variations are present, the results of these studies indicate that neither matching by internal resistance nor by capacity is worthwhile for cells in parallel.

The analysis of initial cell-to-cell variations combined with a reduced upper voltage limit revealed that for initial cell-to-cell variations in internal resistance or capacity of one standard deviation (0.3 mΩ/12.4 mAh, 0.9%/0,8%), the SOHs were higher than the SOH of the comparable single-cell aging study. Initial cell-to-cell variations of two standard deviations resulted in comparable aging behavior. Based on these results and to answer research question three partially, it can be summarized that the effects of initial cell-to-cell variations in internal resistance or capacity do not justify the additional effort of cell matching for cells in parallel before module assembly, provided that the relative coefficients of variation of the respective batch (<1% in this study) are small enough. Furthermore, the fourth research question can be answered to the extent that the influence of initial cell-to-cell variations on both the aging behavior and the long-term cell-to-cell variations of cells in parallel is dominated by the influence of the charging profile, especially by a reduced upper voltage limit.

Future studies should verify the findings for different cell formats and electrode compositions. Specifically, it would be interesting to investigate whether there are maximum relative coefficients of variation up to which initial cell-to-cell variations can be neglected. Additionally, further investigation is required to explain the current distribution, especially regarding the correlation of increasing internal resistances and decreasing cell capacities in combination with altered open-circuit-potentials of the cells. For this purpose, a validated simulation model which includes different aging mechanisms could be developed and used for further analyses. Future studies may also be able to overcome the limitations created by small sample sizes by repeating a smaller selection of these investigations with a larger number of cell pairs. In addition, the effects of varying system parameters, such as the number of cells in parallel on the current distribution and the aging behavior of cells in parallel, can be investigated with the presented measurement method, which should also be the subject of future research.

Acknowledgments

The results presented were achieved in association with an INI.TUM project, funded by the AUDI AG. This work also received funding from the Bavarian Research Foundation of the project OparaBatt (Germany, AZ-1296-17). The support of Sven Friedrich by always keeping an eye on the ongoing measurements is greatly acknowledged.

Appendix

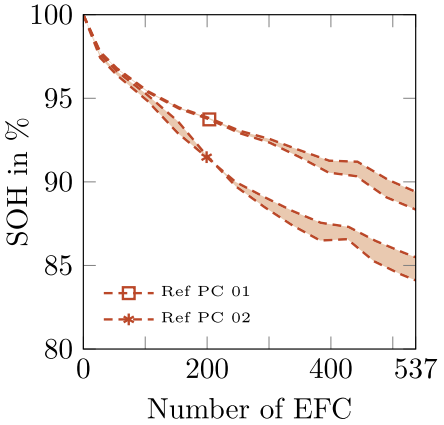

Figure A·1. Aging rates of the reference studies Ref PC 01 and Ref PC 02. Since the cell or the module with the highest aging rate is decisive for the end-of-life of a battery system, Ref PC 02 is chosen as the reference study (Ref PC) for the aging behavior of cells in parallel in this work.

ORCID

Markus Schindler https://orcid.org/0000-0002-3784-6339
Philipp Jocher https://orcid.org/0000-0003-1335-8434
Axel Durdel https://orcid.org/0000-0002-0479-5491
Andreas Jossen https://orcid.org/0000-0003-0964-1405

References

1. M. Schindler, J. Sturm, S. Ludwig, J. Schmitt, and A. Jossen, "Evolution of initial cell-to-cell variations during a three-year production cycle." *eTransportation*, **8**, 100102 (2021).
2. K. Rumpf, M. Naumann, and A. Jossen, "Experimental investigation of parametric cell-to-cell variation and correlation based on 1100 commercial lithium-ion cells." *Journal of Energy Storage*, **14**, 224 (2017).
3. M. Dubarry, N. Vuillaume, and B. Y. Liaw, *Origins and Accommodation of Cell Variations in li-ion Battery Pack Modeling*, **34**, 216 (2010).
4. A. Devie, G. Baure, and M. Dubarry, *Intrinsic Variability in the Degradation of a Batch of Commercial 18 650 Lithium-ion Cells, Energies*, **11**, 1031 (2018).
5. M. Dubarry, C. Truchot, M. Cugnet, B. Y. Liaw, K. Gering, S. Sazhin, D. Jamison, and C. Michelbacher, "Evaluation of Commercial Lithium-ion cells based on Composite Positive Electrode for Plug-in Hybrid Electric Vehicle Applications. Part i: Initial Characterizations." *Journal of Power Sources*, **196**, 10328 (2011).
6. C. Campestrini, P. Keil, S. F. Schuster, and A. Jossen, "Ageing of lithium-ion battery modules with dissipative balancing compared with single-cell ageing." *Journal of Energy Storage*, **6**, 142 (2016).
7. M. Baumann, L. Wildfeuer, S. Rohr, and M. Lienkamp, "Parameter variations within li-ion battery packs–theoretical investigations and experimental quantification." *Journal of Energy Storage*, **18**, 295 (2018).
8. F. An, L. Chen, J. Huang, J. Zhang, and P. Li, "Rate Dependence of Cell-to-cell Variations of Lithium-ion Cells." *Sci. Rep.*, **6**, 35051 (2016).
9. S. Rothgang, T. Baumhofer, and D. U. Sauer, *Diversion of Aging of Battery cells in Automotive Systems, in: 2014 IEEE Vehicle Power and Propulsion Conference (VPPC), IEEE, Piscataway, NJ*, 1 (2014).
10. S. F. Schuster, M. J. Brand, P. Berg, M. Gleissenberger, and A. Jossen, "Lithium-ion cell-to-cell variation during battery electric vehicle operation." *Journal of Power Sources*, **297**, 242 (2015).
11. J. V. Barreras, T. Raj, D. A. Howey, and E. Schaltz, *Results of screening over 200 pristine lithium-ion cells, in: 2017 IEEE Vehicle Power and Propulsion Conference (VPPC), Belfort*, 1 (2017).
12. T. Baumhöfer, M. Brühl, S. Rothgang, and D. U. Sauer, "Production caused variation in capacity aging trend and correlation to initial cell performance." *Journal of Power Sources*, **247**, 332 (2014).
13. M. Dubarry, C. Pastor-Fernández, G. Baure, T. F. Yu, W. D. Widanage, and J. Marco, "Battery energy storage system modeling: investigation of intrinsic cell-to-cell variations." *Journal of Energy Storage*, **23**, 19 (2019).
14. R. Gogoana, M. B. Pinson, M. Z. Bazant, and S. E. Sarma, "Internal resistance matching for parallel-connected lithium-ion cells and impacts on battery pack cycle life." *Journal of Power Sources*, **252**, 8 (2014).
15. D. Oeser, A. Ziegler, and A. Ackva, "Single cell analysis of lithium-ion e-bike batteries aged under various conditions." *Journal of Power Sources*, **397**, 25 (2018).
16. K. Rumpf, A. Rheinfeld, M. Schindler, J. Keil, T. Schua, and A. Jossen, "Influence of cell-to-cell variations on the inhomogeneity of lithium-ion battery modules." *J. Electrochem. Soc.*, **165**, A2587 (2018).
17. M. Schindler, J. Sturm, S. Ludwig, and A. Jossen, "Comprehensive analysis of the aging behavior of nickel-rich, silicon-graphite lithium-ion cells subject to varying temperature and charging profiles." *J. Electrochem. Soc.*, **168**, 060522 (2021).
18. I. Zilberman, S. Ludwig, and A. Jossen, "Cell-to-cell variation of calendar aging and reversible self-discharge in 18 650 nickel-rich, silicon-graphite lithium-ion cells." *Journal of Energy Storage*, **26**, 100900 (2019).
19. S. Miyatake, Y. Susuki, T. Hikihara, S. Itoh, and K. Tanaka, "Discharge characteristics of multicell lithium-ion battery with nonuniform cells." *Journal of Power Sources*, **241**, 736 (2013).
20. M. Schindler, A. Durdel, J. Sturm, P. Jocher, and A. Jossen, "On the impact of internal cross-linking and connection properties on the current distribution in lithium-ion battery modules." *J. Electrochem. Soc.*, **167**, 120542 (2020).
21. M. H. Hofmann, K. Czyrka, M. J. Brand, M. Steinhardt, A. Noel, F. B. Spingler, and A. Jossen, "Dynamics of current distribution within battery cells connected in parallel." *Journal of Energy Storage*, **20**, 120 (2018).
22. A. Fill, S. Koch, A. Pott, and K.-P. Birke, "Current distribution of parallel-connected cells in dependence of cell resistance, capacity and number of parallel cells." *Journal of Power Sources*, **407**, 147 (2018).
23. B. Kenney, K. Darcovich, D. D. MacNeil, and I. J. Davidson, "Modelling the impact of variations in electrode manufacturing on lithium-ion battery modules." *Journal of Power Sources*, **213**, 391 (2012).
24. X. Gong, R. Xiong, and C. C. Mi, "Study of the characteristics of battery packs in electric vehicles with parallel-connected lithium-ion battery cells." *IEEE Transactions on Industry Applications*, **51**, 1872 (2015).
25. S. Santhanagopalan and R. E. White, "Quantifying cell-to-cell variations in lithium ion batteries." *International Journal of Electrochemistry*, **2012**, 1 (2012).
26. P. Jocher, M. Steinhardt, S. Ludwig, M. Schindler, J. Martin, and A. Jossen, "A novel measurement technique for parallel-connected lithium-ion cells with controllable interconnection resistance." *Journal of Power Sources*, **503**, 230030 (2021).
27. F. An, J. Huang, C. Wang, Z. Li, J. Zhang, S. Wang, and P. Li, "Cell sorting for parallel lithium-ion battery systems: Evaluation based on an electric circuit model." *Journal of Energy Storage*, **6**, 195 (2016).
28. M. J. Brand, M. H. Hofmann, M. Steinhardt, S. F. Schuster, and A. Jossen, "Current distribution within parallel-connected battery cells." *Journal of Power Sources*, **334**, 202 (2016).
29. J. Sturm, A. Rheinfeld, I. Zilberman, F. B. Spingler, S. Kosch, F. Frie, and A. Jossen, "Modeling and simulation of inhomogeneities in a 18 650 nickel-rich, silicon-graphite lithium-ion cell during fast charging." *Journal of Power Sources*, **412**, 204 (2019).
30. T. M. M. Heenan, A. Jnawali, M. D. R. Kok, T. G. Tranter, C. Tan, A. Dimitrijevic, R. Jervis, D. J. L. Brett, and P. R. Shearing, "An advanced microstructural and electrochemical datasheet on 18 650 li-ion batteries with nickel-rich nmc811 cathodes and graphite-silicon anodes." *J. Electrochem. Soc.*, **167**, 140530 (2020).
31. LG Chem, Automotive battery, 2019. www.lgchem.com.
32. P. Keil and A. Jossen, "Calendar aging of nca lithium-ion batteries investigated by differential voltage analysis and coulomb tracking." *J. Electrochem. Soc.*, **164**, A6066 (2017).
33. S. Ludwig, I. Zilberman, M. F. Horsche, T. Wohlers, and A. Jossen, "Pulse resistance based online temperature estimation for lithium-ion cells." *Journal of Power Sources*, **490**, 229523 (2021).
34. A. Fill, T. Schmidt, T. Mader, R. Llorente, A. Avdyli, B. Mulder, and K. P. Birke, "Influence of cell parameter differences and dynamic current stresses on the current distribution within parallel-connected lithium-ion cells." *Journal of Energy Storage*, **32**, 101929 (2020).
35. F. M. Kindermann, P. J. Osswald, G. Ehlert, J. Schuster, A. Rheinfeld, and A. Jossen, "Reducing inhomogeneous current density distribution in graphite electrodes by design variation." *J. Electrochem. Soc.*, **164**, E3105 (2017).
36. J. Sturm, A. Frank, A. Rheinfeld, S. V. Erhard, and A. Jossen, "Impact of electrode and cell design on fast charging capabilities of cylindrical lithium-ion batteries." *J. Electrochem. Soc.*, **167**, 130505 (2020).
37. R. Jung, M. Metzger, F. Maglia, C. Stinner, and H. A. Gasteiger, "Oxygen release and its effect on the cycling stability of $\mathrm{lini_xmn_yco_zo_2}$ (nmc) cathode materials for li-ion batteries." *J. Electrochem. Soc.*, **164**, A1361 (2017).
38. K. Richter, T. Waldmann, N. Paul, N. Jobst, R.-G. Scurtu, M. Hofmann, R. Gilles, and M. Wohlfahrt-Mehrens, "Low-temperature charging and aging mechanisms of si/c composite anodes in li-ion batteries: An operando neutron scattering study." *ChemSusChem*, **13**, 529 (2020).
39. P.-F. Lory, B. Mathieu, S. Genies, Y. Reynier, A. Boulineau, W. Hong, and M. Chandesris, "Probing silicon lithiation in silicon-carbon blended anodes with a multi-scale porous electrode model." *J. Electrochem. Soc.*, **167**, 120506 (2020).
40. M. Wetjen, S. Solchenbach, D. Pritzl, J. Hou, V. Tileli, and H. A. Gasteiger, "Morphological changes of silicon nanoparticles and the influence of cutoff potentials in silicon-graphite electrodes." *J. Electrochem. Soc.*, **165**, A1503 (2018).
41. D. Anseán, G. Baure, M. González, I. Cameán, A. B. García, and M. Dubarry, "Mechanistic investigation of silicon-graphite/$\mathrm{lini_{0.8}mn_{0.1}co_{0.1}o_2}$ commercial cells for non-intrusive diagnosis and prognosis." *Journal of Power Sources*, **459**, 227882 (2020).
42. X. Li, A. M. Colclasure, D. P. Finegan, D. Ren, Y. Shi, X. Feng, L. Cao, Y. Yang, and K. Smith, "Degradation mechanisms of high capacity 18 650 cells containing si-graphite anode and nickel-rich nmc cathode." *Electrochimica Acta*, **297**, 1109 (2019).
43. L. Chang, C. Zhang, T. Wang, Z. Yu, N. Cui, B. Duan, and C. Wang, "Correlations of cell-to-cell parameter variations on current and state-of-charge distributions within parallel-connected lithium-ion cells." *Journal of Power Sources*, **437**, 226869 (2019).
44. A. Fill, S. Koch, and K. P. Birke, "Analytical model of the current distribution of parallel-connected battery cells and strings." *Journal of Energy Storage*, **23**, 37 (2019).
45. I. Zilberman, A. Rheinfeld, and A. Jossen, "Uncertainties in entropy due to temperature path dependent voltage hysteresis in li-ion cells." *Journal of Power Sources*, **395**, 179 (2018).